

See discussions, stats, and author profiles for this publication at: <https://www.researchgate.net/publication/231631658>

# Solvent Effects on Hydrogen BondsA Theoretical Study

ARTICLE *in* THE JOURNAL OF PHYSICAL CHEMISTRY A · FEBRUARY 2002

Impact Factor: 2.69 · DOI: 10.1021/jp013677x

CITATIONS

93

READS

19

5 AUTHORS, INCLUDING:



**Adélia J A Aquino**

University of Vienna

93 PUBLICATIONS 1,949 CITATIONS

SEE PROFILE



**Daniel Tunega**

University of Vienna

85 PUBLICATIONS 1,295 CITATIONS

SEE PROFILE



**Georg F. Haberhauer**

University of Natural Resources and Life Scie...

106 PUBLICATIONS 2,420 CITATIONS

SEE PROFILE

## Solvent Effects on Hydrogen Bonds—A Theoretical Study

Adélia J. A. Aquino,<sup>\*,‡,†</sup> Daniel Tunega,<sup>‡,†</sup> Georg Haberhauer,<sup>†</sup> Martin H. Gerzabek,<sup>†</sup> and Hans Lischka<sup>\*,‡</sup>

*Institute for Theoretical Chemistry and Structural Biology, University of Vienna, Währingerstrasse 17, A-1090 Vienna, Austria, and Austrian Research Centers Seibersdorf, A-2444 Seibersdorf, Austria*

*Received: October 2, 2001; In Final Form: November 29, 2001*

Hydrogen-bonded interactions in the acetic acid dimer and in complexes formed by acetic acid with acetaldehyde, acetamide, ammonia, methanol, and phenol and in corresponding complexes between the acetate anion and the same ligands as before were studied in the gas phase and in solution by means of quantum chemical DFT/BLYP calculations. Three solvents (heptane, DMSO, and water) of largely varying polarity were chosen. The polarized continuum model was used for the description of the solvent. Optimized geometries, reaction energies, and Gibbs free energies of complex formation were computed. In the neutral complexes an opening of the weaker of the two hydrogen bonds formed in the complex is observed with increasing polarity of the solvent. This opening is interpreted by the creation of optimal conditions for separate solvation of the subsystems of the hydrogen bond in competition with the geometrical requirements for the formation of this bond. Even though almost all reaction energies are found to be negative, only the strongly bound complexes, acetic acid dimer, and acetic acid-acetamide are stable according to Gibbs free energy results. The main factors for this finding are the entropy loss on the formation of the bimolecular complex and the changes of the free energy of solvation. Solvation effects are interpreted in terms of dipole moments, solvent-accessible surfaces, and cavity volumes of the separate molecules and of the complexes.

### I. Introduction

Hydrogen bonds constitute a very interesting class of intermolecular interactions, which are of extreme importance in many fields of chemistry and molecular biology. Therefore, the properties of hydrogen bonds have been investigated in detail by numerous experimental and theoretical methods (for reviews see refs 1–5). Quantum chemical approaches have been used to analyze the basic bonding properties of hydrogen bonds and to obtain, for example, accurate data about interaction energies, geometry parameters, and vibrational spectra. At present, high-quality theoretical results are available for many systems and we refer to the extended collection given in ref 5 for their discussion. It is interesting to note that most of the theoretical studies have concentrated on the accurate description of isolated complexes such as dimers, trimers, or smaller oligomers, and that at least in *ab initio* calculations further environmental effects on these complexes have been rarely taken into account. However, in natural environments hydrogen bonds will be subject to a large variety of hydrophobic or hydrophilic influences originating from the surrounding into which they are placed. Because of the almost ubiquitous occurrence of hydrogen bonds in nature, these environments could be created, for example, by aqueous solutions, by subsections of proteins in biological systems or in soils (a case in which we are mostly interested in), by organic/inorganic environments of clay surfaces, and organic soil material. A multitude of other scenarios of practical interest are, of course, conceivable as well. In many cases polar surroundings will be derived from water molecules or solvated ions, and apolar environments will come

from aliphatic chains or aromatic substituents. Cases of intermediate polarity will occur, of course, also.

The reason for the concentration of quantum chemical investigations on isolated clusters is the fact that the calculation of solvent effects still poses major problems within these methods. Several approaches are being used for the treatment of solvent effects. In discrete models, solvent molecules are treated explicitly and placed as cluster around the solute. The cluster sizes, which can be treated in this way by *ab initio* methods is rather limited because of the rapidly increasing amount of computational effort. To take into account significantly larger clusters, surrounding solvent shells have to be computed by simpler methods, which lead to mixed quantum mechanical-molecular mechanical (QM-MM) or completely classical models. For a recent review and further references therein, see ref 6. The introduction of classical force fields leads to a significant speed up of calculations. However, the advantage of increased speed is counterbalanced by the difficulty to determine reliable force field parameters.

The explicit consideration of solvent molecules gives detailed insight into solvation complexes, but requires extensive computer resources because of the many particles involved in the calculations. Therefore, as an alternative, continuum models have been developed.<sup>7,8</sup> These methods go back to the classic work by Born,<sup>9</sup> Onsager,<sup>10</sup> and Kirkwood.<sup>11</sup> The progress made in recent solvent models (e.g. PCM, polarized continuum model,<sup>12</sup> COSMO, conductor like screening model,<sup>13</sup> or SM, solvent model<sup>14</sup>) is the treatment of the solute by quantum mechanical methods and a realistic modeling of the solute cavity by overlapping spheres. These methods are much less time-consuming than comparative quantum chemical calculations using explicit solvent molecules and have been applied successfully to the calculation of many solvation processes (see refs 6, 12c, 14c).

\* To whom correspondence should be addressed: E-mail: adelia.aquino@univie.ac.at; hans.lischka@univie.ac.at.

<sup>‡</sup> University of Vienna.

<sup>†</sup> Austrian Research Centers, Seibersdorf.

In this work, we want to use a continuum model for the study of environmental effects on hydrogen bonded systems. Actual choices of molecular systems are derived from our interest in the properties of organic soil constituents such as humic substances and pesticides in which the carboxyl group plays a major role as functional group. Therefore, the acetic acid was chosen as one component in binary complexes and a series of other compounds were selected, which contained as characteristic features carbonyl, amino, and hydroxy groups. Since carboxylic acids occur also in deprotonated form in natural soil environments, interactions with acetate were considered as well. Our list of complexes studied in this work contains several frequently encountered functionalities and should give useful evidence beyond the original context for which the selections were made. To model different environmental situations, three dielectric media of strongly different relative dielectric constants were selected. The three solvents range from strong polarity (water) via dimethyl sulfoxide (DMSO) to the unpolar solvent heptane. One major aim was the computation of geometries and formation energies for the selected complexes subject to various solvent influences. Based on these data, we were interested to find simple interpretations of the observed trends in the computed data in terms of a few characteristic quantities such as dipole moments, charge transfer, solvent-accessible surfaces, and cavity volume. In this way we wanted to arrive at general conclusions, which go beyond the scope of the concrete list of studied interactions.

## II. Computational Methods

The final calculations were performed on the density functional theory (DFT)/BLYP<sup>15</sup> level of theory. Self-consistent field (SCF), DFT/B3LYP,<sup>16</sup> and Møller–Plesset perturbation theory to second order (MP2)<sup>17</sup> calculations were carried out for comparison reasons. The basis sets used in this work were selected as a compromise between reliability of results and computational efficiency. Three basis sets were investigated: 3-21G<sup>18</sup>, split valence polarization (SVP),<sup>19</sup> and SVP+sp. The 3-21G basis set is of double- $\zeta$  quality and was chosen for comparison reasons in view of future calculations on larger molecules. The SVP+sp basis is constructed by augmenting the SVP basis with a set of s and p functions on oxygen, nitrogen, and carbon. The exponents of these additional basis functions were obtained by dividing the smallest respective exponent of the SVP basis set by a factor of 3. As has been shown in test calculations before<sup>20</sup> and will be confirmed by the present results, the basis set superposition error (BSSE) of the SVP basis is reduced substantially by additional s and p functions on heavy atoms. Therefore, the SVP+sp basis is used as our standard basis set. The counterpoise method<sup>21</sup> is used to correct for the BSSE.

Two sets of six different dimers were selected. The first series was formed by acetic acid (AcOH) as one component and acetic acid, acetaldehyde (AcH), methanol (MeOH), phenol (PhOH), ammonia (NH<sub>3</sub>), or acetamide (AcNH<sub>2</sub>) as the other one. All these complexes are neutral and form cyclic structures with two hydrogen bonds in the gas phase. We used these gas-phase structures as starting points for the geometry optimizations in solution and did not consider any further open structures as they have been investigated e.g. by Nakabayashi et al.<sup>22</sup> and Dannenberg et al.<sup>23</sup> for acetic acid dimer. The second series, with the total charge  $-1$ , was composed of the acetate anion (AcO<sup>-</sup>) as one component in interaction with the molecules from the first set. Again, only one of several possible conformers for each charged system was investigated.

Calculations were performed for the isolated systems (gas phase) and for three different solvents – water, DMSO, and heptane with relative dielectric constants  $\epsilon_r = 78.39$ , 46.70, and 1.92, respectively. The PCM approach<sup>12</sup> was used for the description of the solvent continuum. Within this model the solvent–solute interaction energy is composed of a term describing the solute–solvent electrostatic polarization, a dispersion–repulsion term, and the energy needed to form a cavity into which the solute is placed. The electrostatic interaction term is represented by apparent point charges placed on small elements (tesserae) on the cavity surface. The solvent accessible surface of the cavity for the solute is defined as a set of overlapping spheres centered on the nuclei of the solute atoms. The radii of these spheres are obtained from the United Atom Topological Model<sup>24</sup> and are multiplied by scaling factor of 1.2 (recommended value within the PCM model). More information about specific details of the PCM model can be found in ref 24. The computations were carried out using the program package GAUSSIAN 98.<sup>25</sup>

At the beginning, full geometry optimizations were carried out for all monomers and complexes in the gas phase. Then, the solvent with the lowest dielectric constant was switched on and optimization was again performed. These optimized geometries were used as the starting point for the optimization in DMSO. This procedure was also repeated for water. Formation energies of complexes were calculated for both gas and liquid phases as the difference of total energies of the hydrogen-bonded complex and the individual components. Calculated formation energies for different solvents are corrected by BSSE obtained for the gas phase. Harmonic vibrational frequencies and thermodynamic quantities of formations (enthalpies and Gibbs free energies) have been computed for the gas-phase structures within the standard harmonic oscillator/rigid rotator/ideal gas approximation. Thermodynamic quantities are computed for  $T = 298.15$  K. Following previous approaches,<sup>20,26,27</sup> we calculated Gibbs free energies of formations of complexes in solution ( $\Delta G^{\text{sol}}$ ) according to

$$\Delta G^{\text{sol}} = \Delta G^{\text{gas}} + \Delta \Delta G_{\text{solv}} + RT \ln(1/22.4) \quad (1)$$

where  $\Delta G^{\text{gas}}$  is formation Gibbs free energy in the gas phase,  $\Delta \Delta G_{\text{solv}}$  is the difference in free energy of solvation ( $\Delta G_{\text{solv}}$ ) of the complex and respective components. The last term is a correction to the change of reference state from ideal gas to solution.<sup>28</sup> One has to note that especially for strong polar solvents geometries and vibrational modes can differ considerably in comparison to the gas phase. Therefore, the use of zero point energies and thermal contributions taken from gas-phase calculations can cause certain errors in the evaluation of  $\Delta G^{\text{sol}}$ .

## III. Results and Discussions

The selection of the DFT functional and of the basis set were performed on the basis of systematic tests using the SCF, DFT/BLYP, DFT/B3LYP, and MP2 methods and the 3-21G, SVP, and SVP+sp basis sets. These test calculations were carried out for the neutral complexes only. As one can see from the results given in Table 1, it is highly recommendable to use polarization functions in the basis set in agreement with numerous previous results. One observes a considerable difference between 3-21G and SVP interaction energies for all methods used. Differences are not so dramatic between SVP and SVP+sp results. The importance of the additional s and p functions becomes evident when the BSSE is considered. It is given for the BLYP calculations in Table 1 in parentheses also.

**TABLE 1: Interaction Energies (Not Corrected for BSSE) in the Gas Phase for Different Basis Sets and Methods<sup>a</sup>**

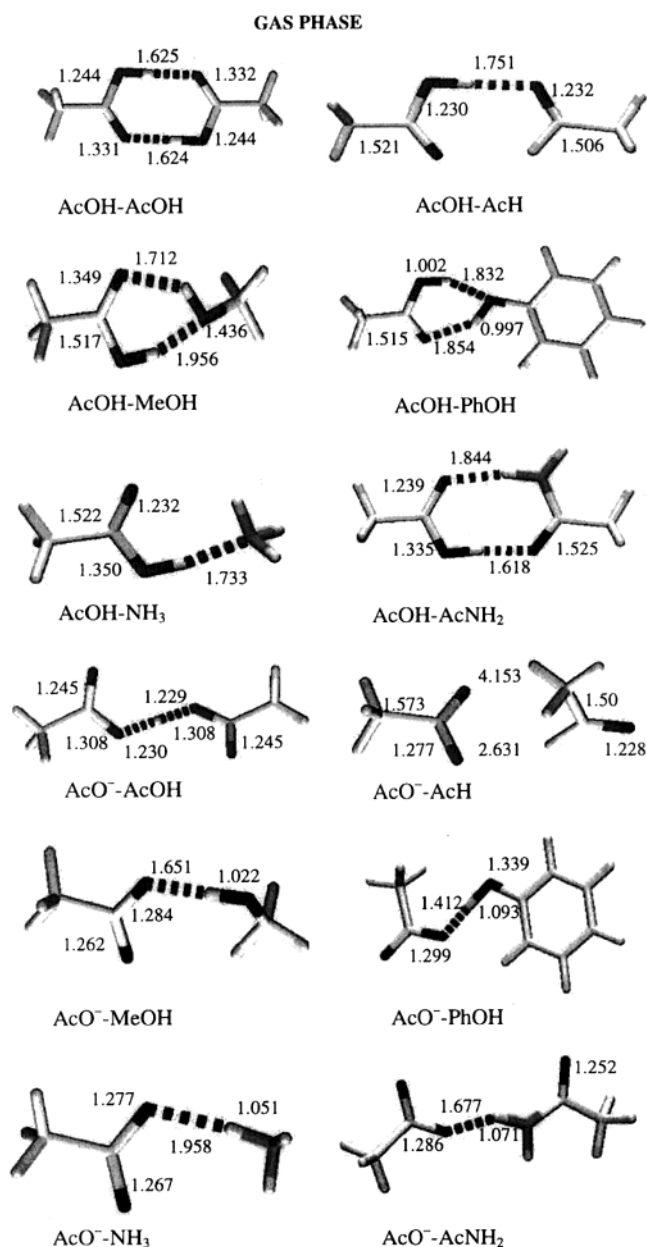
basis set	SCF	BLYP <sup>b</sup>	B3LYP	MP2
Acetic Acid Dimer				
3-21G	-26.9	-34.2 (-14.3)	-34.2	
SVP	-16.4	-21.6 (-6.4)	-21.7	-16.2
SVP+sp	-14.6	-16.5 (-1.2)	-17.6	-17.1
Acetic Acid–Methanol				
3-21G	-20.0	-28.5 (-12.9)	-27.6	
SVP	-18.4	-16.0 (-6.2)	-15.7	-9.9
SVP+sp	-9.3	-10.7 (-1.2)	-9.6	-12.0
Acetic Acid–Ammonia				
3-21G	-19.3	-29.2 (-8.1)	-28.1	
SVP	-11.2	-15.9 (-5.2)	-15.8	-10.5
SVP+sp	-9.0	-11.3 (-1.1)	-11.9	-12.3
Acetic Acid–Acetamide				
3-21G	-25.3	-31.8 (-10.6)	-31.8	
SVP	-15.4	-20.1 (-5.9)	-20.3	-15.2
SVP+sp	-13.9	-15.8 (-0.9)	-16.8	-16.8
Acetic Acid–Acetaldehyde				
3-21G	-16.3	-19.8 (-10.2)	-20.1	
SVP	-9.8	-11.9 (-4.9)	-12.3	-9.8
SVP+sp	-8.6	-8.6 (-0.8)	-9.6	-10.2
Acetic Acid–Phenol				
3-21G	-18.6	-25.3 (-11.2)	-25.0	
SVP	-10.0	-13.7 (-5.0)	-13.8	
SVP+sp	-8.6	-9.4 (-1.1)	-10.3	

<sup>a</sup> All values in kcal/mol. <sup>b</sup> BSSE in parentheses.**TABLE 2: Interaction Energies  $\Delta E$ , Basis Set Superposition Error  $\Delta E_{\text{BSSE}}$ , and BSSE Corrected Interaction Energies  $\Delta E_{\text{corr}}$  Using the BLYP/SVP+sp Approach for the Gas Phase<sup>a</sup>**

system	$\Delta E$	$\Delta E_{\text{BSSE}}$	$\Delta E_{\text{corr}}$
acetic acid dimer	-16.5	-1.2	-15.3
acetic acid–acetaldehyde	-8.6	-0.8	-7.8
acetic acid–methanol	-10.7	-1.2	-9.5
acetic acid–phenol	-8.3	-1.1	-8.3
acetic acid–ammonia	-11.3	-1.1	-10.2
acetic acid–acetamide	-15.8	-0.9	-14.9
acetate–acetic acid	-25.4	-1.0	-24.4
acetate–acetaldehyde	-10.4	-0.6	-9.9
acetate–methanol	-18.5	-0.8	-17.7
acetate–phenol	-27.4	-0.7	-26.7
acetate–ammonia	-9.8	-0.5	-9.4
acetate–acetamide	-24.2	-0.8	-23.4

<sup>a</sup> All values in kcal/mol.

The BSSE amounts to a substantial fraction of the interaction energy (up to 50%) in case of the 3-21G basis set. It is still important for the SVP basis set and reaches acceptable values only for the SVP+sp basis set. In the latter case, the BSSE oscillates around 1 kcal/mol. A comparable BSSE can usually only be achieved by using much larger basis sets.<sup>29</sup> Thus, the SVP+sp basis constitutes a very cost-effective alternative for reducing the BSSE. Taking the MP2/SVP+sp calculations as a reference, both BLYP and B3LYP results deviate only little thereof. The average difference for BLYP/SVP+sp is 1.1 kcal/mol and for B3LYP/SVP+sp it is around 0.8 kcal/mol, respectively. Since BLYP and B3LYP results are very close, we decided to continue in the following calculations with the computationally more efficient BLYP method in combination with the SVP+sp basis set. In Table 2 final interaction energies for the gas phase are given. Table 3 contains optimized geometry parameters characterizing the hydrogen bond formed in the complexes. The Y...H, X–H, and X...Y bond distances and the XHY bond angles of a X–H...Y hydrogen bonds are given. Only the most stable structures found in the present investiga-

**Figure 1.** Structures of neutral and charged complexes in gas phase. Bond distances in Å.

tions are considered. In Figures 1 and 2 optimized structures are displayed for the gas phase and in aqueous solution. BSSE-corrected interaction energies are collected in Table 4 for gas phase and all three solvents considered in this work.

**A. Gas-Phase Results.** All of the selected neutral molecules form two hydrogen bonds with acetic acid. The first hydrogen bond has its origin in the interaction between the carboxyl OH group of the acetic acid and the hydrogen acceptor atom of the partner (O or N). The second hydrogen bond is formed between the carbonyl oxygen atom of the carboxyl group of acetic acid and the hydrogen atom of the partner. This hydrogen atom is of very different origin. For both alcohols (methanol and phenol) it belongs to the hydroxyl group, for acetamide it is the hydrogen atom of the amide group, for acetaldehyde it is that of the aldehyde group, and for ammonia it is one of the three hydrogen atoms. In the acetic acid dimer we have two equivalent hydrogen bonds. In the gas phase, both hydrogen bonds are formed very effectively and the two hydrogen bonds are almost coplanar. Structural information for the two hydrogen bonds is given in Table 3 for all complexes. The first line for each complex refers



TABLE 3: Geometrical Parameters Optimized for Gas and Liquid Phases Using the BLYP/SVP+sp Approach<sup>a</sup>

	gas				heptane				DMSO				water			
	$R_{Y\cdots H}$	$R_{X-H}$	$R_{X\cdots Y}$	$\angle XHY$	$R_{Y\cdots H}$	$R_{X-H}$	$R_{X\cdots Y}$	$\angle XHY$	$R_{Y\cdots H}$	$R_{X-H}$	$R_{X\cdots Y}$	$\angle XHY$	$R_{Y\cdots H}$	$R_{X-H}$	$R_{X\cdots Y}$	$\angle XHY$
AcOH–AcOH	1.624	1.026	2.650	180.0	1.606	1.028	2.634	180.0	1.597	1.029	2.626	178.6	1.599	1.029	2.627	177.9
AcOH–AcH	1.751	1.008	2.579	180.0	1.740	1.008	2.748	179.7	1.738	1.008	2.747	179.6	1.669	1.015	2.667	166.6
	2.450	1.123	3.264	128.0	2.449	1.123	3.257	127.5	2.483	1.123	3.273	126.1	3.126	1.126	3.825	116.6
AcOH–MeOH	1.712	1.013	2.679	157.9	1.692	1.014	2.659	158.0	1.654	1.019	2.635	160.1	1.613	1.024	2.634	174.3
	1.956	0.991	2.762	136.7	1.959	0.991	2.752	135.2	2.011	0.990	2.770	131.6	3.306	0.996	3.375	85.4
AcOH–PhOH	1.832	1.002	2.763	153.2	1.812	1.002	2.742	152.8	1.775	1.005	2.716	154.3	1.686	1.012	2.658	159.7
	1.854	1.000	2.710	142.0	1.828	0.998	2.689	109.5	1.876	0.996	2.699	137.9	2.246	0.990	2.815	115.2
AcOH–NH <sub>3</sub>	1.733	1.028	2.752	170.5	1.687	1.033	2.712	171.1	1.597	1.059	2.656	178.3	1.532	1.088	2.616	172.6
	2.516	1.032	3.118	116.6	2.592	1.032	3.135	112.4	2.885	1.003	3.262	102.2	3.361	1.036	3.473	87.5
AcOH–AcNH <sub>2</sub> <sup>b</sup>	1.618	1.029	2.644	174.9	1.593	1.032	2.622	174.3	1.563	1.038	2.595	172.5	1.553	1.040	2.586	171.6
	1.844	1.043	2.870	167.1	1.844	1.041	2.867	166.1	1.893	1.038	2.910	165.2	1.934	1.360	2.954	164.6
Ac <sup>−</sup> –AcOH	1.229	1.230	2.454	172.4	1.226	1.228	2.449	172.4	1.226	1.227	2.448	172.4	1.225	1.225	2.445	172.4
Ac <sup>−</sup> –AcH	2.631 <sup>c</sup>				2.658				2.897				2.907			
Ac <sup>−</sup> –MeOH	1.651	1.022	2.672	178.6	1.647	1.020	2.667	178.5	1.648	1.016	2.663	177.0	1.667	1.011	2.672	171.8
Ac <sup>−</sup> –PhOH	1.412	1.093	2.504	177.7	1.417	1.088	2.504	178.4	1.438	1.070	2.509	179.7	1.529	1.038	2.560	171.7
Ac <sup>−</sup> –NH <sub>3</sub>	1.958	1.051	3.000	171.0	1.923	1.050	2.971	175.5	1.991	1.043	3.032	175.5	2.099	1.038	3.134	174.8
Ac <sup>−</sup> –AcNH <sub>2</sub>	1.677	1.071	2.746	176.2	1.682	1.067	2.784	176.5	1.722	1.060	2.781	176.4	1.714	1.060	2.771	175.3

<sup>a</sup> First line for each neutral complex refers to the first (stronger) hydrogen bond, second line to the second (weaker) hydrogen bond. For more details see text. <sup>b</sup> First line refers to O–H $\cdots$ O, the second one to O $\cdots$ H–N. <sup>c</sup> Smallest distance between one of the oxygen atoms from acetate and one of the hydrogen atoms from acetaldehyde.

to the first hydrogen bond, and the second line to the second bond (see also Figure 1).

One can see from Figure 1 and the OHX angles given in Table 3 that the shorter of the two hydrogen bonds is almost collinear in most cases, in agreement with the current picture of geometries of hydrogen bonds.<sup>5</sup> Exceptions are observed for complexes containing methanol and phenol. The deviations from linearity found there are due to the fact that the hydroxyl oxygen of the alcohols is involved in both hydrogen bonds. The acetic acid dimer is bound very strongly with short H $\cdots$ O distances of 1.624 Å for both hydrogen bonds. The calculated O $\cdots$ O distances are 2.650 Å, in good agreement with the experimental value of 2.684 Å obtained from gas electron diffraction.<sup>30</sup> Our calculated bond distance is in better agreement with experiment than the value of 2.742 Å obtained at the MP2/6-31G(d) level<sup>31</sup> and a little worse than the value of 2.675 Å obtained from MP2/D95\*\* calculations.<sup>23</sup> Other ab initio investigations<sup>32</sup> using methods and basis sets of comparable quality show similar results for optimized geometry parameters. The calculated formation energy  $\Delta E$  of −15.26 kcal/mol (see Table 4) corresponds to the formation of relatively strong hydrogen bonds. This result is in good agreement with the MP2/6-31G(d) value of −13.5 kcal/mol,<sup>31</sup> the DFT calculations reported by Colominas et al.<sup>27</sup> and the experimental gas-phase formation enthalpy ranging between −14.2 and −15.3 kcal/mol.<sup>33</sup> In the complexes of acetic acid with acetamide, ammonia and acetaldehyde, respectively, the stronger of the two hydrogen bonds is that where the hydroxyl group of the acetic acid is participating. This bond is very strong in the complex acetic acid-acetamide with a length of 1.618 Å. The second hydrogen bond is relatively strong in the acetic acid-acetamide complex also, which is reflected by a bond length of 1.844 Å. For the complexes acetic acid-acetaldehyde and acetic acid-ammonia, the second hydrogen bond is weak with a H $\cdots$ O bond length of about 2.5 Å. The situation for acetic acid-methanol and acetic acid-phenol is different. The hydrogen bond formed between the hydroxyl group of the acetic acid and the oxygen of methanol is weaker than the second one formed between the hydrogen atom of the hydroxyl group of methanol and the carbonyl oxygen of acetic acid (see respective bond distances in Figure 1). In the acetic acid-phenol system the lengths of both hydrogen bonds are very close to each other with bond lengths of about 1.83–1.85 Å. In systems where both hydrogen bonds are short

(acetic acid dimer and acetic acid-acetamide), the interaction energies are also larger in absolute value (about −15 kcal/mol) than in the remaining four neutral complexes with weaker hydrogen bonds, where the interaction energies are found in the interval from −7.8 to −10.2 kcal/mol (see Table 4).

After having optimized gas-phase geometries, vibrational frequencies and thermodynamics contributions to the interaction electronic energies were calculated. Formation enthalpies  $\Delta H$  and free energies  $\Delta G$  for complex formation in gas phase are presented in Table 5. Thermal contributions to  $\Delta H$  amount to about 1–2 kcal/mol, which is of the order of 10–20%. However, the entropic contribution is substantial. We compute for the acetic acid dimer a value of −12.8 kcal/mol for  $T\Delta S$  (see Table 5). The experimental values of the entropy contribution  $T\Delta S$  to the dimerization is about −10.7 kcal/mol<sup>33b–d</sup> and agrees quite well with our result. This large loss of entropy accompanying the dimerization is originated from the transformation of translational and rotational degrees of freedom of the monomers into vibrational ones in the complex. This is a general phenomenon for all associative reactions of type A + B  $\rightarrow$  C<sup>34</sup> (for a detailed analysis of all contributions to the  $\Delta G$  of formation for the water dimer see ref 5). Similar entropy effects for the acetic acid dimer have been calculated by Calominas et al.<sup>27</sup> at the MP2/aug-cc-pVTZ level and by Dannenberg et al.<sup>23</sup> using the MP2/D95\*\* method. The unfavorable  $T\Delta S$  factor causes that only strongly bound complexes (acetic acid dimer and acetic acid-acetamide) are stable in gas phase at room temperature. All the others neutral complexes are unstable according to calculated  $\Delta G$  values.

Optimized geometries of charged systems in gas phase are also shown in Figure 1. The situation is different in comparison to the neutral complexes. In the case of charged complexes, the dominating attractive contribution to the interaction energy is asymptotically of charge–dipole type. Thus, interactions are stronger than in neutral systems where the dipole–dipole interaction prevails. One exception is ammonia, where the complex with the acetate anion is weaker than for the neutral complex with acetic acid. In this case the two structures are not directly comparable since in the neutral complex the hydrogen bond is formed between the hydrogen atom of the hydroxyl group of the acetic acid and the nitrogen atom of the ammonia, while in the charged complex ammonia interacts with the carboxylate through its hydrogen atom. The acetate anion

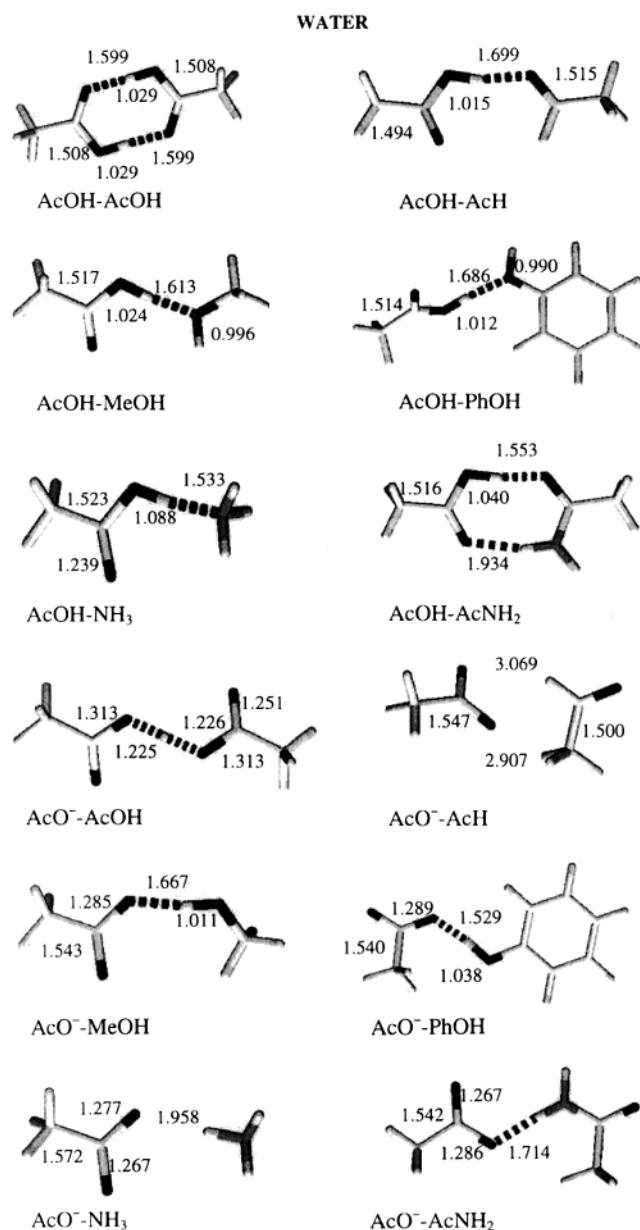


**Figure 2.** Structures of neutral and charged complexes in water. Bond distances in Å.

**TABLE 4: BSSE-Corrected Interaction Energies  $\Delta E$  for Gas and Liquid Phases Using the BLYP/SVP+sp Approach<sup>a</sup>**

system	gas	heptane	DMSO	water
AcOH-AcOH	-15.3	-13.4	-10.1	-2.8
AcOH-AcH	-7.8	-6.7	-4.7	-1.1
AcOH-MeOH	-9.5	-8.0	-5.2	-2.8
AcOH-PhOH	-8.3	-7.1	-3.9	1.6
AcOH-NH <sub>3</sub>	-10.2	-9.7	-8.8	-6.5
AcOH-AcNH <sub>2</sub>	-14.9	-13.0	-9.6	-4.0
AcO <sup>-</sup> -AcOH	-24.4	-16.8	-8.3	-3.9
AcO <sup>-</sup> -AcH	-9.0	-3.6	1.5	1.3
AcO <sup>-</sup> -MeOH	-17.7	-11.6	-5.5	-1.5
AcO <sup>-</sup> -PhOH	-26.7	-17.7	-7.1	-4.8
AcO <sup>-</sup> -NH <sub>3</sub>	-8.6	-5.0	-0.5	0.5
AcO <sup>-</sup> -AcNH <sub>2</sub>	-23.4	-14.4	-4.6	0.0

<sup>a</sup> All values in kcal/mol.

acts as a very strong Brønsted base for protons from partners in the dimers. As mentioned before, we investigated for charged complexes such conformers in which only one hydrogen bond is formed. The strength of this hydrogen bond varies considerably. Acetic acid forms a symmetric hydrogen bond with the

**TABLE 5: Interaction Enthalpies and Gibbs Free Interaction Energies for the Gas Phase and Liquid Phases Using the BLYP/SVP+sp Approach<sup>a</sup>**

	gas		heptane	DMSO	water
system	$\Delta H$	$\Delta G$	$\Delta G$	$\Delta G$	$\Delta G$
AcOH-AcOH	-14.7	-1.9	-1.8	1.4	7.5
AcOH-AcH	-6.2	3.5	2.7	4.8	8.3
AcOH-MeOH	-8.0	1.8	1.6	4.3	6.7
AcOH-PhOH	-6.9	3.1	3.0	6.2	11.2
AcOH-NH <sub>3</sub>	-8.7	0.6	-0.7	0.2	2.4
AcOH-AcNH <sub>2</sub>	-12.8	-3.2	-3.1	1.9	5.9
AcO <sup>-</sup> -AcOH	-25.5	-15.5	-9.7	-1.2	3.1
AcO <sup>-</sup> -AcH	-10.7	-2.4	2.6	9.8	6.9
AcO <sup>-</sup> -MeOH	-16.6	-7.8	-3.5	2.6	6.6
AcO <sup>-</sup> -PhOH	-26.5	-16.5	-9.3	1.3	3.6
AcO <sup>-</sup> -NH <sub>3</sub>	-8.0	-0.8	1.8	6.3	6.5
AcO <sup>-</sup> -AcNH <sub>2</sub>	-22.0	-12.0	-4.8	5.1	9.6

<sup>a</sup> All values in kcal/mol.

acetate anion (see Figure 1, structure 7) where the proton is located in the middle between the two oxygen atoms of the respective carboxylate groups. The interaction is one of the strongest with an interaction energy of -24.39 kcal/mol. Another conformer was investigated in the work of Meot-Ner et al.<sup>35</sup> where an additional weak hydrogen bond between one hydrogen atom of the methyl group of acetic acid and the second oxygen atom of the carboxylate group of acetate was formed. The formation enthalpy of -27.7 kcal/mol obtained at the MP2/6-31G\* level for this complex is slightly larger (in absolute value) than the value of -25.5 kcal/mol obtained for the acetic acid-acetate complex of this work (Table 5). Relatively weak interactions are observed in gas phase for the acetate-acetaldehyde and acetate-ammonia systems with formation energies of -9.0 and -8.6 kcal/mol, respectively (see Table 4). In these cases, one finds also larger interatomic distances in the hydrogen bonds (see Table 3). This is due to the fact that ammonia and acetaldehyde are weaker proton donors. The other three complexes form strongly bound systems with interaction energies of about -20 kcal/mol or more (in absolute value) similar to the acetate-acetic acid complex. The strongest interaction is observed for the acetate/phenol complex, which is in opposition to the corresponding neutral system. The amount of the destabilizing effect of entropy is for charged complexes similar to the neutral one (compare respective  $\Delta H$  and  $\Delta G$  values in Table 5). However, since interaction energies are generally more negative for charged complexes as compared to the neutral ones,  $\Delta G$  values are negative in this case. This means that all charged complexes are predicted to be stable at room temperature in the gas phase.

**B. Solvent Results.** As mentioned before, the effects of three solvents—heptane, DMSO, and water—have been investigated. Since major components of the interaction energy in hydrogen bonds are electrostatic and of charge-transfer nature,<sup>5</sup> a pronounced effect of the polarity of the solvent on hydrogen bond strength is expected. Geometries of complexes optimized in different solvents are characterized in Table 3 and depicted in Figure 2 for water as solvent. Neutral complexes will be discussed first. As was observed in the gas phase, these complexes contain—except for the acetic acid dimer—two different kinds of hydrogen bonds. The hydrogen bond, which is stronger in the gas-phase becomes even shorter under the solvent effect. Thus, these hydrogen bonds are stabilized with increasing polarity of the solvent. This is illustrated in Figure 3, where Y...H hydrogen bond distances are plotted. Changes in these bond distances range from 0.025 Å (acetic acid dimer) to 0.20 Å (acetic acid-ammonia). In line with the decrease of

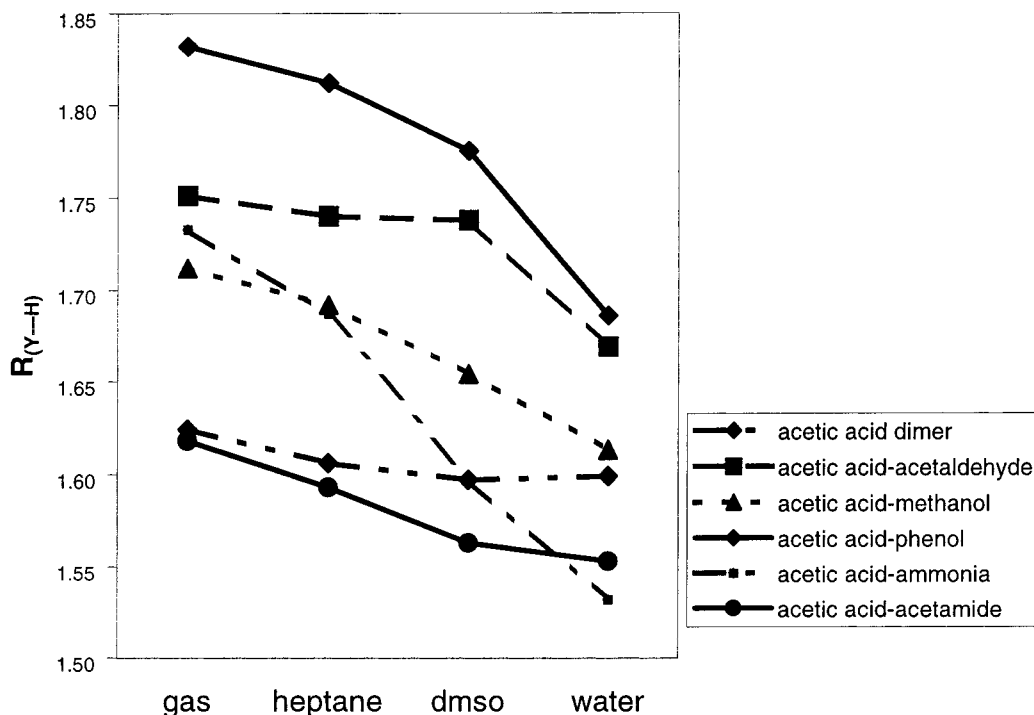


Figure 3. Hydrogen bond distances  $Y\cdots H$  (Å) of the stronger hydrogen bond for neutral complexes in gas and liquid phases.

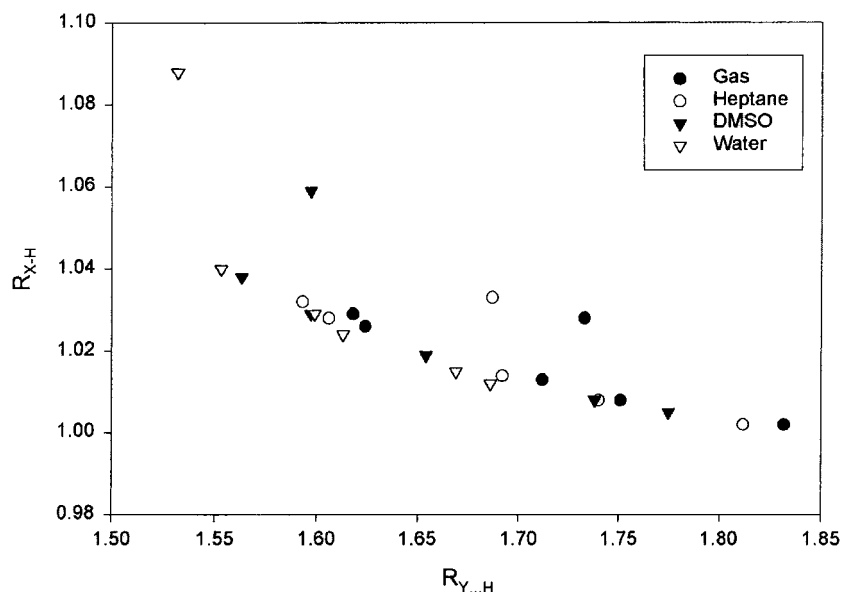
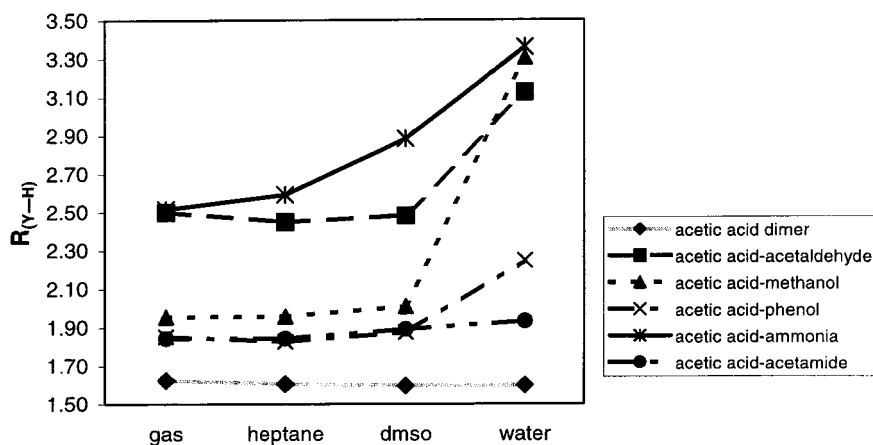


Figure 4. Correlation between the  $X-H$  bond length and the  $Y\cdots H$  distance for the stronger hydrogen bond for neutral complexes in the gas phase and the three solvents investigated in this work.

the hydrogen bond distance, the  $X-H$  distances increase (0.003 Å for acetic acid dimer to 0.060 Å for acetic acid-ammonia). Such correlation between  $Y\cdots H$  and  $X-H$  is typical for hydrogen bonded systems and are displayed, for example, for data collected from X-ray and neutron scattering experiments on hydrogen bonded crystals in ref 36. Figure 4 shows an analogous analysis for our data. One can see that the correlation between  $X-H$  and  $Y\cdots H$  is very well fulfilled for all four environments. The four points shifted up in Figure 4 belong to the complex  $AcOH-NH_3$ . This shift reflects the different chemical nature of  $Y$  atom in the  $Y\cdots H-X$  bond (nitrogen in this case) as opposed to oxygen in all other cases. Unfortunately, a direct comparison of our results with experimental ones in solution is not possible because of lack of data. Similar trends

in the geometry of hydrogen bonded complexes (decrease of the  $Y\cdots H$  bond and increase of the  $X-H$  bond) as the ones found in this work can also be observed in the series starting from the dimer via oligomer clusters to infinite chains. This systematic behavior based on cooperativity (nonadditivity) effects has, for example, been discussed by Karpfen<sup>37</sup> in case of clusters of hydrogen cyanide and hydrogen fluoride. It has been shown by Chalasinski et al.<sup>38</sup> for the water trimer as example that these nonadditivity effects originate largely from electric polarization at the SCF level which are also included in the PCM model. Therefore, we suggest that similar polarization effects could be responsible for the shortening of the strong hydrogen bonds found in our PCM calculations, where the cluster of discrete molecules is replaced by a continuum.



**Figure 5.** Hydrogen bond distances  $Y\cdots H$  (Å) of the weaker hydrogen bond for neutral complexes in gas and liquid phases.

The second, longer and weaker hydrogen bond behaves differently than the stronger one. With increasing strength of the solvent, these weaker hydrogen bonds generally start to open (see Figure 5). This opening decreases the interaction of this hydrogen bond but improves the possibilities for individual solvation of  $X-H$  and  $Y$  subsystems by increasing the solvent-accessible surface. The bond lengths of the hydrogen bonds of some of these complexes do not increase monotonically with increasing solvent polarity. This is documented in Table 3 and Figure 5. One can see that for the acetic acid-acetaldehyde complex the  $O\cdots H$  bond length of the weaker bond slightly decreases in solvents of weak and medium polarity (heptane and DMSO) and only in the water environment it opens significantly. Similar strong opening in water is also observed for the complexes acetic acid-ammonia, acetic acid-methanol and acetic acid-phenol. The acetic acid dimer and the acetic acid-acetamide complex behave differently in comparison to the other systems, since they both possess two strong hydrogen bonds. One finds in these cases only a small dependence of the  $O\cdots H$  bond length on the polarity of the solvent.

From these results we conclude that the polar solvent environment stabilizes the strong hydrogen bonds in the investigated neutral complexes while weak hydrogen bonds behave differently and can even be broken under the effect of the solvent. Similar conclusions have been made by Sneddon et al.<sup>39</sup> in their molecular mechanics simulations of formamide dimers in different solvents. They showed that hydrogen bonds are more easily broken in the polar solvent than in the apolar one.

Calculated interaction energies for the neutral complexes in different solvents are collected in Table 4 and shown graphically in Figure 6. The interaction energies are significantly decreasing in absolute value with increasing polarity of the solvent. The largest decrease is observed for the two complexes acetic acid dimer and acetic acid-acetamide, where relatively strong hydrogen bonds had been observed before. The reduction in the strength of the interaction amounts to more than 10 kcal/mol when comparing gas-phase results with those of the water environment. Nakabayashi et al.<sup>22</sup> observed a similar decrease of the formation energy (about 13 kcal/mol) for the cyclic acetic acid dimer at the HF/DZP level and using the RISM-SCF model for the water solvent.

Despite the aforementioned strengthening of hydrogen bonds by polar solvents in terms of bond distances, there are other factors, which lead to an energetic destabilization of the complexes in comparison to the separated systems. Since the energetic stability of a complex is computed as the energy

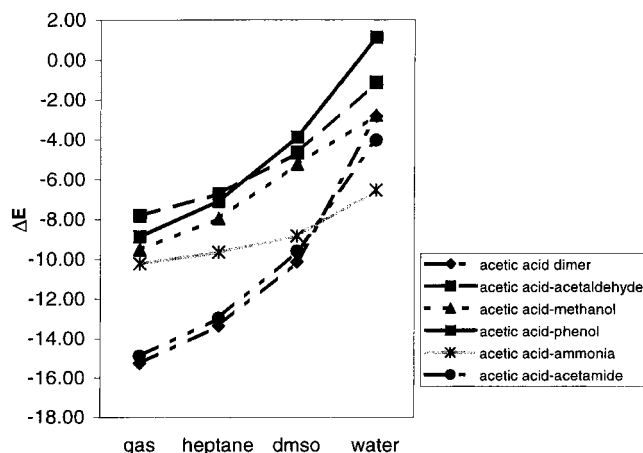


**Figure 6.** Interaction energies  $\Delta E$  (kcal/mol) of neutral complexes in gas and liquid phases.

**TABLE 6: Solvation Free Energies  $\Delta G_{\text{solv}}$  for Different Solvents Using the BLYP/SVP+sp Approach<sup>a</sup>**

system	heptane	DMSO	water
AcOH-AcOH	-1.7	-0.5	-1.9
AcOH-AcH	-1.8	-1.1	-5.8
AcOH-MeOH	-1.8	-1.1	-6.9
AcOH-PhOH	-3.0	-2.4	-11.8
AcOH-NH <sub>3</sub>	-3.8	-4.5	-11.1
AcOH-AcNH <sub>2</sub>	-2.8	-2.9	-6.7
AcO <sup>-</sup> -AcOH	-24.1	-49.6	-60.1
AcO <sup>-</sup> -AcH	-23.9	-52.0	-63.4
AcO <sup>-</sup> -MeOH	-25.5	-54.3	-58.0
AcO <sup>-</sup> -PhOH	-24.0	-47.6	-64.9
AcO <sup>-</sup> -NH <sub>3</sub>	-27.5	-58.6	-71.4
AcO <sup>-</sup> -AcNH <sub>2</sub>	-23.5	-48.0	-53.5
AcO <sup>-</sup>	-31.2	-54.3	-73.2
AcOH	-2.2	-3.2	-7.8
AcH	-1.7	-2.2	-4.1
MeOH	-2.0	-3.0	-5.1
PhOH	-3.8	-5.6	-11.1
NH <sub>3</sub>	-1.6	-2.6	-5.2
AcNH <sub>2</sub>	-3.3	-5.7	-10.2

<sup>a</sup> All values in kcal/mol.

difference between the energy of this complex in a solvent cavity surrounded by the solvent medium and analogous energies for the separated components embedded in the solvent, it is instructive to compare solvation energies for the complex and the individual components. These data are collected in Table 6. For all cases investigated here the sum of the solvation energies of the monomers is larger in absolute value than the solvation energies of the corresponding complex. This fact is

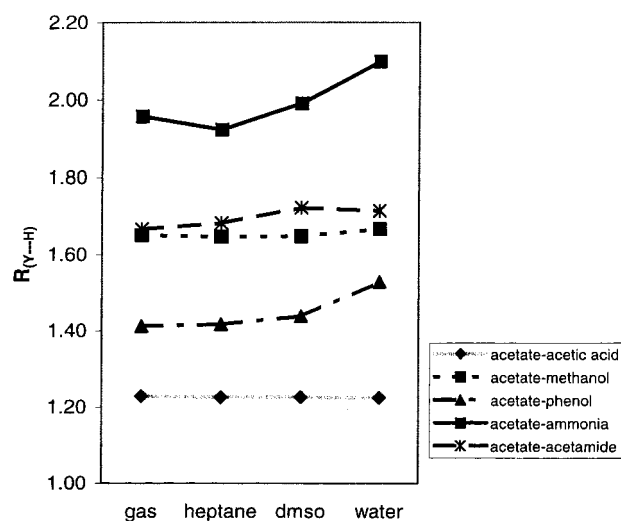


**TABLE 7: Comparison of Selected Properties of Hydrogen-Bonded Complexes and Individual Components**

system	$\mu$ [D]	surface (S) [ $\text{\AA}^2$ ]	volume (V) [ $\text{\AA}^3$ ]	S/V [ $\text{\AA}^{-1}$ ]
AcOH–AcOH	0.19	181.2	174.6	1.04
AcOH–AcH	3.84	183.1	169.5	1.08
AcOH–MeOH	3.89	164.6	150.8	1.09
AcOH–PhOH	5.04	219.2	208.5	1.05
AcOH–NH <sub>3</sub>	5.42	142.0	124.8	1.14
AcOH–AcNH <sub>2</sub>	4.02	185.7	178.7	1.04
AcO <sup>−</sup> –AcOH		186.2	167.4	1.11
AcO <sup>−</sup> –AcH		181.1	164.1	1.10
AcO <sup>−</sup> –MeOH		161.1	140.1	1.15
AcO <sup>−</sup> –PhOH		205.2	196.0	1.05
AcO <sup>−</sup> –NH <sub>3</sub>		142.2	118.6	1.20
AcO <sup>−</sup> –AcNH <sub>2</sub>		186.8	172.8	1.08
AcO <sup>−</sup>		94.8	78.5	1.21
AcOH	2.30	105.5	90.6	1.16
AcH	4.00	98.9	82.6	1.20
MeOH	2.27	78.2	63.0	1.24
PhOH	2.36	130.6	119.4	1.09
NH <sub>3</sub>	2.24	56.7	40.1	1.41
AcNH <sub>2</sub>	5.50	108.5	94.3	1.15

related to different volumes and surface areas of the solute cavities and to dipole moments of monomers and complexes. Respective data are presented in Table 7 for water as the strongest polar solvent. All neutral compounds have large dipole moments and each of these molecules possesses a polar functional group, which interacts strongly with polar solvents. Thus all these monomers have relatively high solvation energies. Even in heptane a substantial attractive solvation effect is observed. The polar functional groups of the monomers are always involved in the formation of dimers. Therefore, they are at least partially not available for interaction with the solvent. Mainly nonpolar, hydrophobic functional groups, such as CH<sub>3</sub> remain fully available for contacts with solvents. Moreover, due to the formation of complexes the solvent-accessible surface is generally decreased in comparison with the isolated monomers by about 7–14% (see Table 7). The reduction of the surface accessible area is expressed in Table 7 also in terms of the ratio of molecular surface to volume (S/V). The reduced availability of the polar groups for interaction with the solvent and the reduction of the surface area on complexes formation leads quite generally to a reduction of solvation energies (in absolute value) for the complexes and, thus, to a relative destabilization with respect to the monomers. This effect is most pronounced for water as solvent.

Additional, specific cancellations of dipole moments in the complexes may occur, which can also disfavor the solvation properties of the complexes. This effect is most evident in the acetic acid dimer, where mainly for geometry reasons the total dipole moment of the complex is practically zero even though the isolated acetic acid has a dipole moment of 2.3 D (Table 7). The others five neutral complexes have relatively high dipole moments, which favor solvation by polar solvents. However, the global effects (e.g. solvent-accessible surface) mentioned before lead to a total reduction of the solvation energies of these complexes with respect to the corresponding individual components also. Nakabayashi et al.<sup>22</sup> and Luque et al.<sup>27</sup> observed similar effects for cyclic acetic acid dimer. Moreover, Nakabayashi et al.<sup>22</sup> also tested two other possible conformers of the acetic acid dimer (linear, forming only one hydrogen bond and side-on, where one hydroxyl group of one acetic acid forms two hydrogen bonds with the carboxyl group of the other acetic acid molecule). It was shown that both of them are less stable than the cyclic dimer in the gas phase. Owing to the large dipole moments of these structures (about 4 D in the gas phase) it was

**Figure 7.** Hydrogen bond distances  $Y\cdots H$  ( $\text{\AA}$ ) of the charged complexes in gas and liquid phases.

expected that both complexes could be very stable in a polar solvent. In fact, interpretation of Raman spectra of binary solutions of acetic acid and water<sup>40</sup> demonstrate the existence of open chain clusters. However, despite this fact, Nakabayashi et al.<sup>22</sup> found from their RISM-SCF HF/DZP calculations that also in aqueous solution both open dimers are less stable than the cyclic one.

In Table 5  $\Delta G$  values of formation calculated according to eq 1 are listed for all complexes in the three solvents. One can see that most of the  $\Delta G$  values for neutral complexes are positive. In the gas phase and in heptane, the acetic acid dimer and acetic acid-acetamide complex display negative  $\Delta G$  values. Additionally, the acetic acid-ammonia complex shows a negative value in heptane as well. Thus, only these complexes are predicted to be stable in these environments. The experimental<sup>41</sup> free energy of formation for acetic acid dimer in chloroform is about  $-2.4$  kcal/mol. This value is comparable to our calculated  $\Delta G$  of  $-1.7$  kcal/mol for heptane as solvent, since chloroform is also an apolar solvent with a relative dielectric constant  $\epsilon_r$  of 4.9. The estimated experimental free formation energies for the acetic acid dimer in water solution are in the range 0.0–1.7 kcal/mol.<sup>42</sup> This differs significantly from our calculated value of 7.5 kcal/mol. Colominas et al.<sup>27</sup> published similar, somewhat lower values around 4–5 kcal/mol based on continuum models as well as on free-energy perturbation calculations. This discrepancy between experimental and theoretical results has been taken as an indication that the experimentally observed acetic acid dimers in aqueous solutions are not cyclic as observed in gas phase or in apolar solvents.<sup>27</sup> Other structures (linear and side-on, see above) have been suggested by Nakabayashi et al.,<sup>22</sup> but no conclusive answer has been given so far.

Selected geometrical parameters describing the hydrogen bonds of charged systems in solution are documented in Table 3. Figure 2 contains additional geometry parameters in water as solvent. As it was mentioned before, there is only one hydrogen bond in the charged complexes. Figure 7 shows the solvent dependence of the  $Y\cdots H$  hydrogen bond distances involved in the hydrogen bond. Only smaller changes are observed in this figure except for the acetate-ammonia complex. This behavior is different in comparison to the neutral systems (see Figure 3). Mutual orientation of the interacting molecules in the complexes does not change significantly from gas to the water environment (compare Figures 1 and 2).

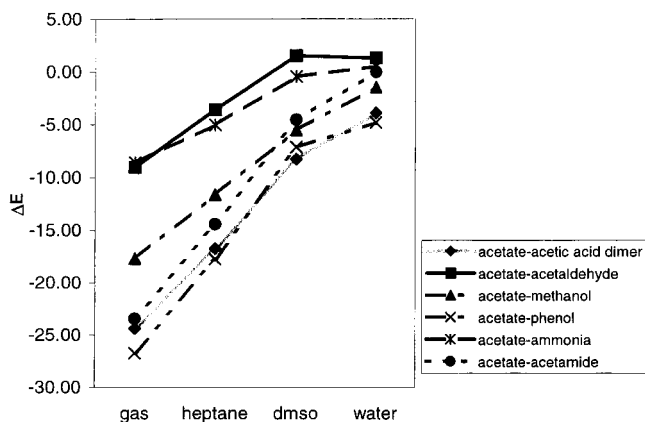


**Figure 8.** Interaction energies (kcal/mol) of the charged complexes in gas and liquid phases.

Calculated interaction energies for charged dimers are presented in Table 4. The same decrease (in absolute value) with increasing polarity of the solvent is observed as for the neutral systems. As depicted in Figure 8,  $\Delta E$  decreases in absolute value from gas phase to aqueous solution for each complex. For acetate-acetaldehyde in DMSO and water and for acetate-ammonia in water we obtained positive  $\Delta E$  values. This means that these structures are unstable with respect to the solvated, isolated systems. The decrease of  $\Delta E$  in absolute value with increasing solvent polarity can be explained similarly to the neutral systems. In Table 6 the surface accessible area, molecular volume and  $S/V$  ratio is given for charged complexes and respective monomers in aqueous solution. As for the neutral complexes, the sum of the surfaces for isolated molecules is larger than the surface of the corresponding complex and part of the hydrophilic region of monomers is involved in hydrogen bonds and thus is not available for interaction with the solvent. Thermodynamic properties are collected in Table 5. Since some of the interaction energies are strongly negative, they show also negative  $\Delta G$  values in heptane (see Table 5). Because of positive free energies none of the charged complexes are stable in DMSO or in water.

#### IV. Conclusions

Hydrogen bonds between several polar molecules and the acetic acid molecule and/or the acetate anion, respectively, have been investigated using DFT theory. Comparison of BLYP, B3LYP, and MP2 results and also comparison to previously published results obtained at the MP2 level with extended basis sets<sup>22,23,27</sup> showed that combination of the BLYP functional with the SVP+sp basis set is very efficient for obtaining results of reasonable quality. It was also shown that the effect of the basis set superposition error on the formation energies substantially decreases using the SVP+sp basis set. The effects of three solvents (heptane, DMSO, water) of different polar strength on the formation of complexes have been analyzed.

Calculations of enthalpies and free energies of formation of complexes in the gas phase showed that only strongly bound systems (with strongly negative formation enthalpies) are able to offset the high entropy loss during the formation of bimolecular complexes. From the neutral systems, these are only the acetic acid dimer and the acetic acid-acetamide complex. This pronounced stability is due to the fact that in both cases cyclic complexes are formed with two relatively strong hydrogen bonds. The remaining neutral systems investigated here have one stronger and one weaker hydrogen bond and the effect of

$T\Delta S$  of formation makes  $\Delta G$  positive. The enthalpies of formation of the charged complexes are more negative than for neutral complexes since the interactions are of charge–dipole nature. Thus, all of these charged systems are predicted to be stable in the gas-phase according to calculated free energies of the formation.

Analysis of the solvent effect showed several factors affecting the stabilization of complexes in different polar environments. Shortening of the strong hydrogen bonds with increasing polar strength of solvents indicates increased stabilization of these bonds. On the other hand, the weaker hydrogen bonds in the cyclic, neutral dimers open under the effect of the strong polar solvent. Thus, the interaction within these hydrogen bonds decreases with increasing polarity of the solvent. The reason for this opening seems to be the creation of optimal conditions for separate solvation of the X–H and Y subsystems of a X–H...Y hydrogen bond in competition with the geometrical requirements for the formation of this hydrogen bond in the complex. Calculated free energies of formation in solution show that only the strongly bound complexes in weak-polar environment are stable. Results for medium (DMSO) and strong (water) polar solvents indicate that the formation of bimolecular complexes is not favorable (except the acetic acid-acetate complex in DMSO). The reason for this is found in the balance between the solvation energies of the separated molecules and the complexes. The separated molecules have a large solvation energy since they are either charged or possess big dipole moments. The solvation energy of the complexes is always smaller than the sum of solvation energies of individual components (in absolute value). As a consequence, the  $\Delta\Delta G_{\text{solv}}$  contribution to  $\Delta G$  of formation in solution is positive.  $\Delta\Delta G_{\text{solv}}$  increases with increasing polar strength of the solvent. An explanation of this effect was found in the decrease of the attractive part and an increase of the nonattractive part of the solvent-accessible surface area of the bimolecular complexes for polar solvents in comparison with individual components since the attractive surface area is “locked” in the formed hydrogen bonds between molecules in complexes. This destabilizing effect of  $\Delta\Delta G_{\text{solv}}$  is a general one for formation of bimolecular hydrogen-bonded complexes in polar solvents.

**Acknowledgment.** This work was supported by the Austrian Science Fund, project no. P12969-CHE and by a Hertha-Firnberg fellowship. We are grateful for technical support and computer time at the DEC Alpha server of the computer center of the University of Vienna.

#### References and Notes

- (1) Schuster, P.; Zundel, G.; Sandorfy, C. *The Hydrogen Bond. Recent Developments in Theory and Experiments*, I–III; Elsevier/North-Holland: New York, 1976.
- (2) *Molecular Interactions*, Vol. 1; Ratajczak, H.; Orville-Thomas, W. J., Eds.; Wiley & Sons: New York, 1980.
- (3) Hobza, P.; Zahradník, R. *Intermolecular Complexes*; Elsevier Science: New York, 1988.
- (4) Jeffrey, G. A. *An Introduction to Hydrogen Bonding*; Oxford University Press: New York, 1997.
- (5) Scheiner, S. *Hydrogen Bonding. A Theoretical Perspective*; Oxford University Press: New York, 1997.
- (6) Orozco, M.; Luque, F. J. *Chem. Rev.* **2000**, *100*, 4187.
- (7) Tomasi, J. *Theor. Chem. Acc.* **2000**, *103*, 196.
- (8) Luque, F. J.; López, J. M.; Orozco, M. *Theor. Chem. Acc.* **2000**, *103*, 343.
- (9) Born, M. *Z. Phys.* **1920**, *1*, 45.
- (10) Onsager, L. *J. Am. Chem. Soc.* **1936**, *58*, 1486.
- (11) Kirkwood, J. J. *J. Chem. Phys.* **1935**, *3*, 300.
- (12) (a) Miertus, S.; Scrocco E.; Tomasi, J. *J. Chem. Phys.* **1981**, *55*, 117. (b) Miertus S.; Tomasi, J. *J. Chem. Phys.* **1982**, *65*, 239. (c) Tomasi, J.; Persico,

- M. *Chem. Rev.* **1994**, 94, 2027. (d) Cossi, M.; Barone, V.; Camini, R.; Tomasi, J. *Chem. Phys. Lett.* **1996**, 255, 327.
- (13) (a) Klamt, A.; Schüürmann, G. *J. Chem. Soc., Perkin Trans.* **1993**, 2, 799. (b) Truong, T. N.; Stefanovich, E. V. *J. Chem. Phys.* **1995**, 103, 3709.
- (14) (a) Cramer, C. J.; Truhlar, D. G. *J. Am. Chem. Soc.* **1991**, 113, 8305. (b) Cramer, C. J.; Truhlar, D. G. *Science* **1992**, 256, 213. (c) Cramer, C. J.; Truhlar, D. G. *Chem. Rev.* **1999**, 99, 2161.
- (15) (a) Becke, A. D. *Phys. Rev. A* **1988**, 38, 3098. (b) Lee, C.; Yang, W.; Parr, R. G. *Phys. Rev. B* **1988**, 37, 785. (c) Miehlich, B.; Savin, A.; Stoll, H.; Preuss, H. *Chem. Phys. Lett.* **1989**, 157, 200.
- (16) Becke, A. D. *J. Chem. Phys.* **1993**, 98, 5648.
- (17) Head-Gordon, M.; Pople, J. A.; Frisch, M. J. *Chem. Phys. Lett.* **1988**, 153, 503.
- (18) (a) Binkley, J. S.; Pople, J. A.; Hehre, W. J. *J. Am. Chem. Soc.* **1980**, 102, 939. (b) Gordon, M. S.; Binkley, J. S.; Pople, J. A.; Pietro, W. J.; Hehre, W. J. *J. Am. Chem. Soc.* **1982**, 104, 2797. (c) Pietro, W. J.; Francel, M. M.; Hehre, W. J.; Defrees, D. J.; Pople, J. A.; Binkley, J. S. *J. Am. Chem. Soc.* **1982**, 104, 5093.
- (19) (a) Schäfer, A.; Horn, H.; Ahlrichs, R. *J. Chem. Phys.* **1992**, 97, 2571. (b) Schäfer, A.; Huber, C.; Ahlrichs, R. *J. Chem. Phys.* **1994**, 100, 5829.
- (20) Tunega, D.; Habershauer, G.; Gerzabek, M.; Lischka, H. *J. Phys. Chem.* **2000**, 104, 6824.
- (21) Boys, S. F.; Bernardi, F. *Mol. Phys.* **1970**, 19, 553.
- (22) Nakabayashi, T.; Sato, H.; Hirata, F.; Nishi, N. *J. Phys. Chem. A* **2001**, 105, 245.
- (23) Dannenberg, J. J.; Paraskevas, L.-R.; Sharma, V. *J. Phys. Chem. A* **2000**, 103, 6617.
- (24) Barone, V.; Cossi, M.; Tomasi, J. *J. Chem. Phys.* **1997**, 107, 3210.
- (25) Frisch, M. J.; Trucks, G. W.; Schlegel, H. B.; Scuseria, G. E.; Robb, M. A.; Cheeseman, J. R.; Zakrzewski, V. G.; Montgomery, J. A., Jr.; Stratmann, R. E.; Burant, J. C.; Dapprich, S.; Millam, V.; Daniels, A. D.; Kudin, K. N.; Strain, M. C.; Farkas, O.; Tomasi, J.; Barone, V.; Cossi, M.; Cammi, R.; Mennucci, C.; Pomelli, C.; Adamo, S.; Clifford, J.; Ochterski, G. A.; Petersson, P. Y.; Ayala, B.; Cui, Q.; Morokuma, K.; Malick, D. K.; Rabuck, A. D.; Raghavachari, K.; Foresman, J. B.; Cioslowski, J.; Ortiz, J. V.; Stefanov, B. B.; Liu, G.; Liashenko, A.; Piskorz, P.; Komaromi, I.; Gomperts, R.; Martin, R. L.; Fox, D. J.; Keith, T.; Al-Laham, M. A.; Peng, C. Y.; Nanayakkara, A.; Gonzalez, C.; Challacombe, M.; Gill, P. M. W.; Johnson, B.; Chen, W.; Wong, M. W.; Andres, J. L.; Head-Gordon, M.; Replogle, E. S.; Pople, J. A. *Gaussian98*, Revision A.7; Gaussian, Inc.: Pittsburgh, PA, 1998.
- (26) (a) Aquino, A. J. A.; Tunega, D.; Harberhauer, G.; Gerzabek, M.; Lischka, H. *Phys. Chem. Chem. Phys.* **2000**, 2, 2845. (b) Aquino, A. J. A.; Tunega, D.; Harberhauer, G.; Gerzabek, M.; Lischka, H. *Phys. Chem. Chem. Phys.* **2001**, 3, 1979.
- (27) Colominas, C.; Teixidó, J.; Cemeli, J.; Luque, F. J.; Orozco, M. *J. Chem. Phys. B* **1998**, 102, 2269.
- (28) Cieplak, P.; Kollman, P. A. *J. Am. Chem. Soc.* **1988**, 110, 3734.
- (29) Rappé, A. K.; Bernstein, E. R. *J. Phys. Chem. A* **2000**, 104, 6117.
- (30) Derissen, J. L. *J. Mol. Struct.* **1971**, 7, 67.
- (31) Dannenberg, J. J.; Paraskevas, L.-R.; Sharma, V. *J. Phys. Chem. A* **2000**, 103, 6617.
- (32) (a) Turi, L.; Dannenberg, J. J. *J. Phys. Chem.* **1993**, 97, 12197. (b) Borisenko, K. B.; Bock, C. W.; Hargittai, I. *J. Mol. Struct. (THEOCHEM)* **1995**, 332, 161. (c) Dannenberg, J. J. *J. Mol. Struct. (THEOCHEM)* **1997**, 401, 279. (d) Burneau, A.; Génin, F.; Quilès, F. *Phys. Chem. Chem. Phys.* **2000**, 2, 5020.
- (33) (a) Mathews, D. M.; Sheets, B. N. *J. Chem. Soc. A* **1969**, 2203. (b) Frurip, D. J.; Curtiss, L. A.; Blander, M. *J. Am. Chem. Soc.* **1980**, 102, 2610. (c) Winkler, A.; Behl, J. B.; Hess, P. *J. Chem. Phys.* **1994**, 100, 2717. (d) Chao, J.; Zwolinski, J. *J. Phys. Chem. Ref. Data* **1978**, 7, 363.
- (34) Searle, M. S.; Williams, D. H. *J. Am. Chem. Soc.* **1992**, 114, 10690.
- (35) Meot-Ner (Mautner), M.; Elmore, D. E.; Scheiner, S. *J. Am. Chem. Soc.* **1999**, 121, 7625.
- (36) Olovsson, I.; Jönsson, P.-G. In *The Hydrogen Bond. Recent Developments in Theory and Experiments*, II; Schuster, P., Zundel, G., Sandorfy, C., Eds.; Elsevier/North-Holland: New York, 1976; p 393.
- (37) Karpfen, A. In *Molecular Interactions*; Scheiner, S., Ed.; John Wiley & Sons: New York, 1997; p 265.
- (38) Chalasinski, G.; Szczesniak, M. M.; Cieplak, P.; Scheiner, S. *J. Chem. Phys.* **1991**, 94, 2873.
- (39) Sneddon, S. F.; Tobias, D. J.; Brooks, C. L., III. *J. Mol. Biol.* **1989**, 209, 817.
- (40) Nakabayashi, T.; Kosugi, K.; Nishi, N. *J. Phys. Chem. A* **1999**, 103, 8595.
- (41) Fujii, Y.; Yamada, H.; Mizuta, M. *J. Phys. Chem.* **1988**, 92, 6768.
- (42) (a) Ng, J. B.; Shurvell, H. F. *J. Phys. Chem.* **1987**, 91, 496. (b) Yamamoto, K.; Nishi, N. *J. Am. Chem. Soc.* **1990**, 112, 549.